Investigating functionalized active coated nano-particles for use in nano-sensing applications

Joshua A. Gordon[1*], Richard W. Ziolkowski[2, 1]

[1]*College of Optical Sciences, University of Arizona, Tucson, AZ 85721*
[2]*Department of Electrical and Computer Engineering University of Arizona, Tucson, AZ 85721*
**Corresponding Author: gordonj@email.arizona.edu*

Abstract: In this paper we investigate the use of active coated nano-particles (CNPs) for nano-sensing applications. Simulation results of the optical properties of an active CNP with a 24nm radius active silica core and 6nm thick plasmonic shell made of silver that has been functionalized by an additional spherical outer layer of varying thickness and refractive index are presented. In particular, the effects of the functional-layer thickness and refractive index on the super-resonant (SR) state of the active CNP are presented. It is shown that the wavelength and optical gain required to excite the SR state may provide *both* a spectral and a power signature usable for nano-scale sensing and that these signatures may be used to identify the dimensions and optical properties of the functional layer. These results are then applied to the case of a functional layer containing a solution of human hemoglobin. It is demonstrated that the concentration of hemoglobin may be remotely determined from these SR signatures.

OCIS codes: (170.4580) Medical optics and biotechnology: Optical diagnostics for medicine; (350.4238) Nanophotonics; (290.4020) Mie Theory; (999.999) Metamaterials

References and Links

1. J. A. Gordon and R. W. Ziolkowski, "The design and simulated performance of a coated nano-particle laser," Opt. Express **15**, 2622 (2007).
2. J. Homola, S. Yee, and G, Gauglitz, "Surface plasmon resonance sensors: review," Sens. Actuators B **54**, 3 (1999).
3. A. W. H. Lin, N. J. Halas, and R. A. Drezek, "Optically tunable nanoparticle contrast agents for early cancer detection: model-based analysis of gold nanoshells," J. Biomed. Opt. **10**, 064035 (2005).
4. L. R. Hirsch and A. M. Gobin, "Metal nanoshells," Ann. Biomed. Eng. **34**, 15 (2006).
5. R. D. Averitt, S. L. Westcott, and N. J Halas, "Linear optical properties of gold nanoshells," J. Opt. Soc. Am. B. **16**, 1824 (1999).
6. J. B. Jackson and N. J. Halas, "Silver nanoshells: variations in morphologies and optical properties," J. Phys. Chem. B **105**, 2743 (2001).
7. M. Friebel and M. Meinke, "Model function to calculate the refractive index of native hemoglobin in the wavelength range of 250-1100nm dependent on concentration," Appl. Opt. **45,** 2838 (2006)
8. G. M. Hale and M. R. Querry, "Optical Constants of Water in the 200-nm to 200-um Wavelength Region," Appl. Opt. **12,** 555 (1973).
9. J. A. Stratton, *Electromagnetic Theory*, (McGraw-Hill New York, 1941).
10. A. L. Aden and M. Kerker, "Scattering of electromagnetic waves from two concentric spheres," J. Appl. Phys. **22**, 1242 (1951).
11. U. Kreibig and M. Vollmer, *Optical Properties of Metal Clusters* (Springer, New York, 1995).
12. P. B. Johnson and R. W. Christy, "Optical constants of the noble metals," Phys. Rev. B **6,** 4370 (1972).

1. Introduction

In sensing applications on the nanometer scale, quantities of measurable interest include the dimensions and refractive index of nano-objects. For example, the sizes and optical properties of biological cells would have an immediate impact on identifying whether a set of cells was

#85628 - $15.00 USD Received 23 Jul 2007; revised 21 Aug 2007; accepted 31 Aug 2007; published 17 Sep 2007

friendly or hostile to an organism. It would be desirable for such nano-sensors to be able to resolve the distance and time scales involved and to have high sensitivities to minute changes in their local environments.

In this paper we investigate the optical properties of a highly resonant nanometer-sized *active* dielectric sphere that is coated with a silver plasmonic shell and surrounded by a dielectric layer of some thickness and refractive index. This basic active coated nano-particle (CNP) was studied extensively in [1]. The additional outer functional layer is used to represent a single or a set of nano-sized objects that surrounds the active CNP. It is sensed by its influence on the optical properties of the un-functionalized, but active CNP. We present results from simulations that are used to investigate the optical properties of a functionalized active CNP when it is immersed in a medium representing an aqueous solution and having a refractive index of 1.33 similar to that of distilled water. Comparisons are made to its response in free space. We will highlight the resulting optical signatures that may be applicable for nano-sensing applications. In particular, the case of an active CNP that has been functionalized by the hemoglobin found in human red blood cells is explored; and it is shown that the concentration of hemoglobin may be determined remotely from the scattering data.

Current plasmon-based sensors that are used in biosensing applications exploit surface plasmon waves (SPWs). In contrast, the proposed CNP-based sensor derives its characteristics from localized surface plasmons (LSPs). In contrast to SPWs, which are bound propagating waves, the LSPs are not propagating waves; they are localized coupled oscillations of the electrons in the plasmonic shell and the electric field exciting it. The SPW-based sensors are typically planar or waveguide devices which are many orders of magnitude larger than the compounds and molecules they are designed to sense. Moreover, due to the momentum difference between the SPW and the exciting optical field, a SPW sensor cannot be driven directly. The SPWs can only be excited by introducing a prism, a waveguide or a more complicated planar grating structure to match the momentum of the optical field to theirs, i.e., they can only be driven if an evanescent wave coupling device is introduced [2]. These large scale SPW-based devices only provide for the detection of spatially integrated changes to the sensing environment. Thus, they are more suited to *in vitro* biosensing applications. On the other hand, in the proposed CNP-based sensors, the LSPs are confined to the surface of a spherical plasmonic shell. Therefore, the physics associated with and the implementations of CNPs for sensing applications are different from those of the SPW-based sensors. For instance, the LSP nature of a CNP sensor allows for direct coupling of the exciting field to the LSPs. Moreover, because of their localized geometry, the CNP sensors can also be designed with sizes ranging from tens of nanometers to a few hundred. This localized feature enables the CNP-based devices to have the capability of spatially resolving the sensing environment in which they have been dispersed. Consequently, it can be envisioned that the CNP-based sensors may be used to target specific regions of interest, particularly within or immediately near a living organism for ***in vivo*** biosensing applications. It is also noted that the SPW-based sensor requires a TM-polarized excitation field and, hence, it is restricted to applications that can accommodate this polarization. In contrast, there is no polarization restriction on the exciting field for the proposed spherical CNP-based sensor. Finally, another desirable characteristic of the proposed CNP-based sensors is the field strength achievable with the associated super resonant lasing states [1], which are excited and monitored as their main signature. The super resonant state inherently provides optical amplification and thus the signal to noise ratio (SNR) in the CNP-based sensor has the potential to be made large. In contrast, the SNR is a major issue for SPW-based devices because of their inherent large evanescent-wave conversion inefficiencies and the large absorption losses associated with the SPWs as they propagate.

Recent work has investigated the use of optically tunable, resonant *passive* plasmonic nano-spheres for biomedical and optical applications. Projected uses for these nano-shells

#85628 - $15.00 USD Received 23 Jul 2007; revised 21 Aug 2007; accepted 31 Aug 2007; published 17 Sep 2007

range from exploiting their tunability for contrast agents in early cancer detection [3, 4]; for drug delivery, and for the creation of near infrared, highly absorbing particles for use in a photo thermal ablation therapy for cancer treatment [3]. Optically tunable plasmonic CNPs have been successfully synthesized with spherical dielectric cores surrounded by thin metallic coatings of silver or gold for a number of years. Dielectric-core gold CNPs have been successfully synthesized, and their optical tunability has been verified experimentally [5]. In these particles the gold nano-shells have thicknesses as thin as 2nm and surround a gold sulfide, AuS_2, core. Tunability from 550nm to 950nm has been demonstrated using particle radii ranging from 4nm to 17nm, respectively. Tunable gold nano-shells made with a silica core have also been successfully synthesized and their optical properties experimentally verified [4]. Tunability has been demonstrated for larger spheres with a 60nm core size and shell thicknesses ranging from 5nm to 20nm to cover the wavelength range from 750nm to 1000nm. The gold-based CNP resonances were observed to shift to longer wavelengths as the core to shell radius ratio increased. In addition, silver coated silica nano-shells with core radii of 40-250nm and shell thicknesses of 10-30nm have also been successfully synthesized and their optical properties have been experimentally verified [6]**.** It has been demonstrated that these silver-silica CNPs exhibit tunable plasmon resonances at shorter wavelengths with a 10% larger enhancement than for the corresponding gold-silica CNPs and, therefore, that they can be used to cover a wider portion of the optical spectrum. In contrast to these investigations and applications of *passive* CNPs, the research presented here explicitly explores the properties and applications of *active* CNPs.

2. Blood model

To simulate the response of the active CNP in the presence of a solution of oxygenated hemoglobin, the linear model developed in [7] is used for the real part of its complex refractive index. This refractive index model is dependent on the hemoglobin concentration. It describes the refractive index of a solution representative of the substances within a human red blood cell in the presence of oxygenated hemoglobin concentrations ranging from 0 to 29 g/dL. This model can be extrapolated with high accuracy to values within the normal human body range of 30 to 36 g/dL. The model for the real part of the refractive index takes the form,

$$n_{Hb}(\lambda, c_{Hb}) = n_{H_2O}(\lambda)[\beta(\lambda)c_{Hb} + 1] \tag{1}$$

where $\beta(\lambda)$ is the specific refractive increment, c_{Hb} is the concentration of hemoglobin and $n_{H_2O}(\lambda)$ is the refractive index of water. These parameter values were obtained over the simulation wavelength range of interest from [7] and [8] for the specific refractive increment and the refractive index of water, respectively. The refractive index of water over the wavelengths of interest is shown in Fig. 1 and the index of the hemoglobin solution for various concentrations that are representative of those used in the following simulations is plotted in Fig. 2.

#85628 - $15.00 USD Received 23 Jul 2007; revised 21 Aug 2007; accepted 31 Aug 2007; published 17 Sep 2007

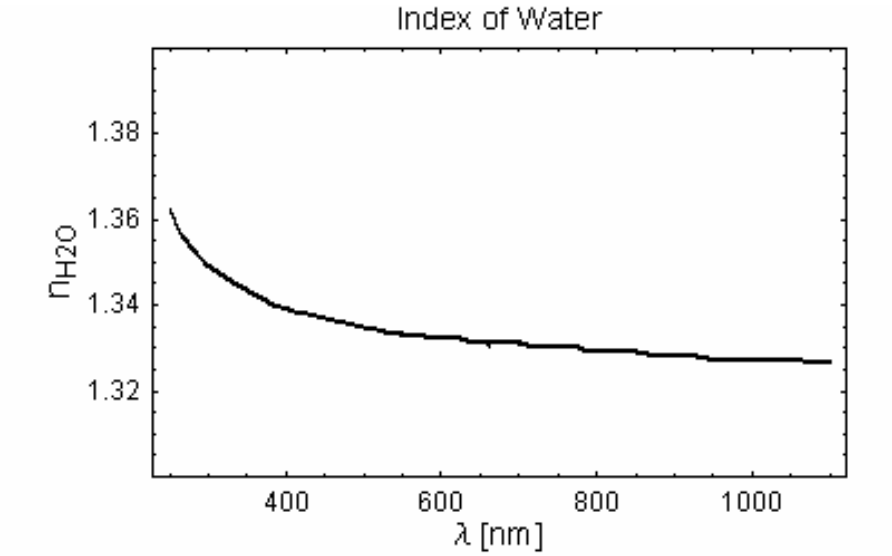

Fig. 1. The index of refraction of water over the wavelength range from 250nm to 1100nm.

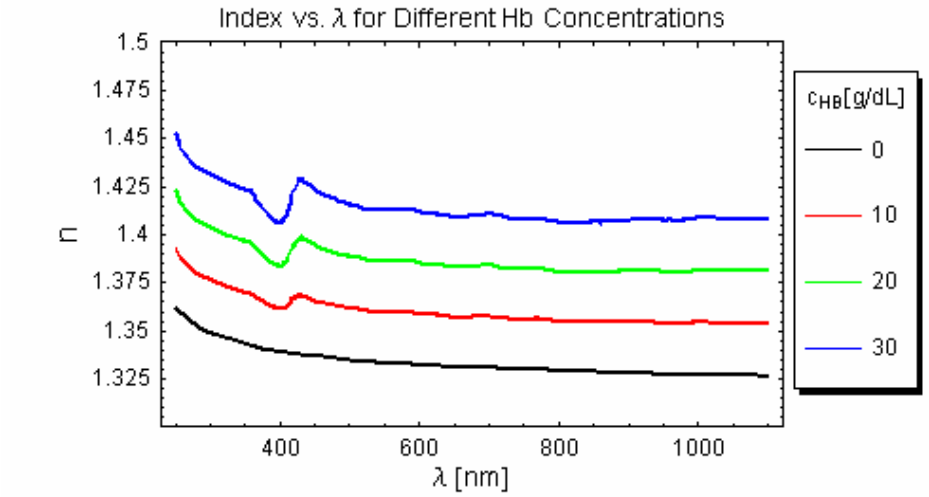

Fig. 2. The index of refraction of hemoglobin solution for different concentrations of hemoglobin, C_{Hb} , over the wavelength range from 250nm to 1100nm.

#85628 - $15.00 USD Received 23 Jul 2007; revised 21 Aug 2007; accepted 31 Aug 2007; published 17 Sep 2007

3. Scattering problem

The optical properties of the active CNP are determined by calculating the scattered field that results from an incident linearly polarized monochromatic plane wave. The scattering geometry is depicted in Fig. 3. All of the materials are assumed to be homogeneous, isotropic and non-magnetic, i.e., $\mu_i = 1$ for $i = 1,...,4$. The incident plane wave travels in a medium that is described by the permittivity ε_4 and permeability μ_4 and that surrounds the CNP. The basic CNP is covered with an additional material layer defined by the radii R_2 and R_3 of its inner and outer boundaries, respectively. This layer is the one to be detected for the proposed sensor applications; it is described by the permittivity ε_3 and permeability μ_3. The active CNP is represented by the layered sphere bounded by R_2. The latter is defined by a core whose outer radius is R_1 and by the permittivity ε_1 and permeability μ_1. It is surrounded with a plasmonic shell defined by the permittivity ε_2 and permeability μ_2 and by the radii R_1 and R_2 of its inner and outer boundaries, respectively. The core permittivity in the absence of gain takes on the value for silica, SiO_2, which is $\varepsilon_1 = 2.05\,\varepsilon_0$. In our investigation the simulations were performed assuming that the dimensions of the active CNP were R_1=24nm and R_2=30nm and, thus, that the plasmonic shell had a thickness equal to 6nm.

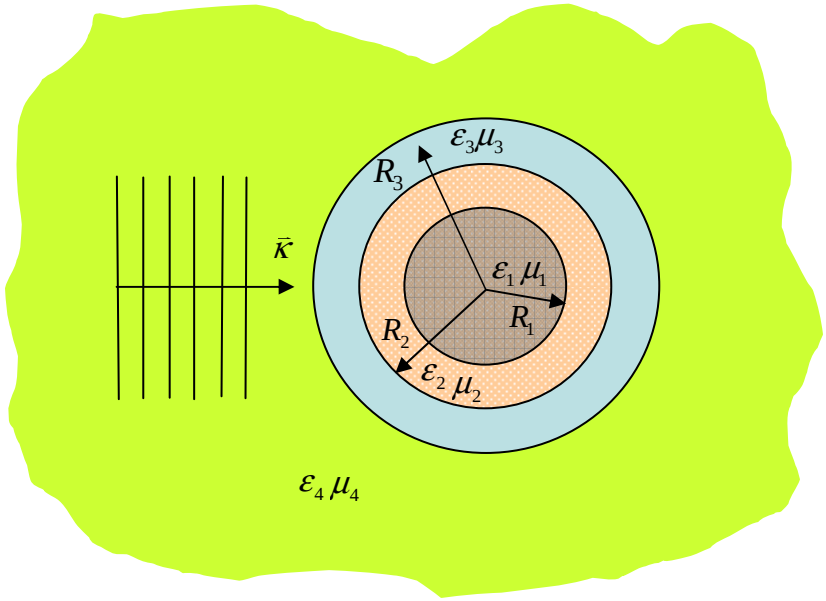

Fig. 3. Plane wave scattering from a multilayered sphere: For the active CNP the core region, defined by ε_1, μ_1, is an active material and the second layer, defined by ε_2, μ_2, is a plasmonic material. The outer third layer, defined by ε_3, μ_3, is the functional layer. The particle is immersed in a host medium, defined by ε_4, μ_4.

#85628 - $15.00 USD Received 23 Jul 2007; revised 21 Aug 2007; accepted 31 Aug 2007; published 17 Sep 2007

For a linearly polarized plane wave incident on a concentrically layered spherical particle, the electric and magnetic fields in each region can be expanded into transverse electric (TE) and transverse magnetic (TM) vector spherical harmonics denoted, respectively, as $\vec{m}(\rho,\theta,\phi)$ and $\vec{n}(\rho,\theta,\phi)$ [9, 10]. The scattered electric and magnetic field in each region, for instance, can then be written in the form

$$\vec{E}_{scat} = E_o \sum_{n=1}^{\infty} (-i)^n \frac{2n+1}{n(n+1)} [a_n \vec{m}_{o1n}^{(3)}(\rho,\theta,\phi) + i b_n \vec{n}_{e1n}^{(3)}(\rho,\theta,\phi)] \tag{2}$$

$$\vec{H}_{scat} = -E_o \sqrt{\varepsilon_4} \sqrt{\mu_4} \sum_{n=1}^{\infty} (-i)^n \frac{2n+1}{n(n+1)} [b_n \vec{m}_{e1n}^{(3)}(\rho,\theta,\phi) - i a_n \vec{n}_{o1n}^{(3)}(\rho,\theta,\phi)] \tag{3}$$

Enforcing the electromagnetic boundary conditions, i.e., the continuity of the tangential electric and magnetic fields at each interface between each material region, a matrix system of equations for the scattered TE and TM field coefficients, respectively, a_n and b_n, is obtained and solved.

The scattering cross-section and absorption cross-section are defined from the scattered and incident fields via Poynting's vector. The scattering cross-section is defined as the total integrated power contained in the scattered field normalized by the irradiance of the incident field. The absorption cross-section is defined by the net power flux through a surface surrounding the concentric shells normalized by the incident field irradiance, and is thus a measure of how much energy is absorbed by the concentric shell structure. Consequently, the total scattering cross-section, absorption cross-section and extinction cross-section are defined from the ratio of the scattered or absorbed power to the incident irradiance, I_{inc}, and can be expressed in terms of the scattered field coefficients as:

$$\sigma_{scat} = \frac{P_{scat}}{I_{inc}} = \frac{2\pi}{\kappa^2} \sum_{n}^{\infty} (2n+1) \left(|a_n|^2 + |b_n|^2 \right) \tag{4}$$

$$\sigma_{abs} = \frac{P_{abs}}{I_{inc}} = -\frac{2\pi}{\kappa^2} \sum_{n}^{\infty} (2n+1) \left(\mathrm{Re}\{a_n\} + |a_n|^2 + \mathrm{Re}\{b_n\} + |b_n|^2 \right) \tag{5}$$

$$\sigma_{ext} = \sigma_{scat} + \sigma_{abs} \tag{6}$$

where $\kappa = 2\pi/\lambda$, with λ is the wavelength in the surrounding medium. The corresponding scattering and absorption efficiencies are defined as the cross sections normalized by the geometric cross section of the particle.

$$Q_{scat} = \frac{\sigma_{scat}}{\pi r^2} \tag{7}$$

#85628 - $15.00 USD Received 23 Jul 2007; revised 21 Aug 2007; accepted 31 Aug 2007; published 17 Sep 2007

$$Q_{abs} = \frac{\sigma_{abs}}{\pi r^2} \tag{8}$$

$$Q_{ext} = Q_{scat} + Q_{abs} \tag{9}$$

As was shown in [1], the extinction cross section of the passive CNPs is dominated by absorption in the size regime of the particles studied here. It was also shown that for the nanometer dimensions of the plasmonic shell under consideration, any neglect of the size dependence of the permittivity by using either a bulk material model or a simple Drude model leads to erroneous results. In particular, these simplistic models ignore significant effects such as size dependent broadening and diminished resonance strength. Consequently, the size dependencies of the plasmonic shell material were included in the models used in the following simulations. To include this size dependence, the dielectric function of the plasmonic material was modified by imposing the mean free path effect in the Drude component of the dielectric function by introducing a size dependent damping frequency [11]. Therefore the total electric response of the plasmonic shell due to both interband transitions and Drude electrons can be described as,

$$\varepsilon(\omega, R) = \varepsilon_{Drude}(\omega, R) + \chi_{IntBand}(\omega) \tag{10}$$

$$\varepsilon_{Drude}(\omega, R) = 1 - \frac{\omega_p^{\,2}}{\Gamma(R)^2 + \omega^2} + i\,\frac{\Gamma(R)^2\,\omega_p^{\,2}}{\omega(\Gamma(R)^2 + \omega^2)} \tag{11}$$

where ω_p and Γ are, respectively, the plasma and collision frequencies. The half width of the resonance

$$\Gamma(R) = \Gamma_\infty + \frac{\mathrm{A}\,\mathrm{V}_F}{R} \tag{12}$$

where A is a constant term assumed to be approximately unity, i.e., $A \sim 1$. The term $\mathrm{V_F}$ is the Fermi velocity.

It was shown in [1] that when gain is introduced into the core of the passive CNP, the losses associated with the plasmonic shell and the core could be overcome. It was also demonstrated that new and enhanced resonance characteristics could be realized which differ from those associated with the passive CNP. In particular it was shown that with the addition of gain in the core, the absorption efficiency may become negative while narrowing from hundreds of nanometers to a few nanometers. This behavior was shown to be indicative of light amplification over an extremely narrow frequency range; it demonstrated the presence of a super resonance (SR) lasing state for the active CNP. A comparison of the scattering and absorption resonances of the un-functionalized passive and active CNP near SR is shown in Fig. 4.

#85628 - $15.00 USD Received 23 Jul 2007; revised 21 Aug 2007; accepted 31 Aug 2007; published 17 Sep 2007

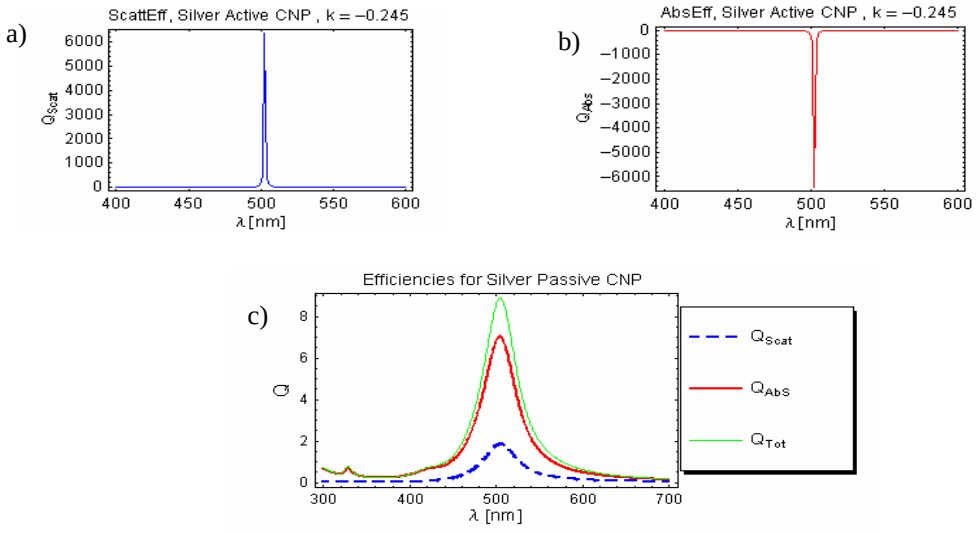

Fig. 4. (a). Super resonant scattering from an *active* CNP, (b) Super resonant emission from an *active* CNP, (c) Absorption dominated scattering in a *passive* CNP.

In the following, the use of the SR state is explored as a highly emissive signature for use in sensing applications on the nano scale. To realize an active CNP in the following simulations, gain was introduced into the core material through the permittivity via a complex refractive index which incorporates a canonical gain model,

$$\varepsilon_{core} = n^2 - k^2 + i2kn \tag{13}$$

where n and k are, respectively, the real and imaginary parts of the refractive index. For optical gain the imaginary part of the refractive index k takes on negative values, i.e., optical gain occurs when $k < 0$.

In Figs. 4(a) and 4(b) the scattering and absorption resonances for the active silver CNP are shown near the SR where the gain term approaches k = -0.245. The scattering, absorption, and total efficiencies associated with this passive resonance are shown in Fig. 4(c). It is obvious that in the passive case the resonance is absorption dominated and broad with a width of approximately 100nm. In the active case the resonance is enhanced several orders of magnitude having a width of only a few nanometers accompanied by negative absorption efficiency values, which indicates emission of radiation and signifies a lasing state.

4. Simulations of functionalized CNPs

The simulations presented below investigate the change in optical properties of the SR state as described above and in [1], when an active CNP is functionalized by an outer layer of some material having a thickness which is on the order of tens of nanometers. The scattering from this functionalized CNP is investigated for two kinds of parameter variations in this outer layer. These variations are the refractive index or the thickness of this layer. As these parameters are varied, the SR state is monitored for any characteristics that differ from those identified for the un-functionalized active CNP. In particular, it will be shown that in the presence of the functional layer, the resonance wavelength and the amount of optical gain required to excite the SR are functions of both its index and thickness. We have chosen to focus on the SR state as an optical signature for nano-scale sensing because 1) it is highly

#85628 - $15.00 USD Received 23 Jul 2007; revised 21 Aug 2007; accepted 31 Aug 2007; published 17 Sep 2007

emissive, i.e. a non-absorbing high output signature; 2) it is extremely narrow; and 3) it is spectrally and gain tunable depending on changes in the local environment.

The following numerical experiments investigate the tunability of the SR state of an active CNP consisting of a 24nm radius spherical active silica core encased in a 6nm thick plasmonic shell of silver and surrounded by a layer of lossless dielectric of variable thickness. The bulk material constants used for silver in these simulations were obtained from [12]. In practical situations this functional layer may represent a molecule or some other nano-scaled object having a similar dimension and real refractive index. The thickness of the outer dielectric layer was varied from 2nm to 10nm in 2nm increments; its real refractive index, n_3, was varied independently from 1.0 to 2.0 in increments of 0.2. While the index was varied, the thickness was held constant at a value of $t = 10nm$. When the thickness was varied, the outer layer index was held fixed at a value of $n_3 = 1.7$. For each set of thickness and index values the scattering coefficients were calculated across the wavelength range of 300nm to 1000nm in 1nm increments. The optical gain coefficient in the active silica core was varied for the cases when the particle was in either an air environment or a water environment. The optical gain was varied over a range suitable to observe scattering in both the resonant absorption and emission regimes of the active CNP. For each thickness and index value the gain required to achieve the SR state, as well as the wavelength at which it occurs, was then determined. This process is visualized in Fig. 5 for the specific case of an active CNP functionalized by a 10nm thick layer of index 1.7 and immersed in lossless water of index 1.33. As shown in Fig. 5(a), the SR state is defined by the peak in the gain spectrum of the absorption efficiency, $|Q_{abs}(k,\lambda)|$. The corresponding wavelengths of the maxima of $|Q_{abs}(k,\lambda)|$ as a function of the gain are plotted in Fig. 5(b). These plots are generated by determining first the peak value of $|Q_{abs}(k,\lambda)|$ across the simulation wavelength range for a set of gain parameter values, k, and then plotting the maximum efficiency magnitude and the corresponding resonance wavelength against the gain value used to obtain that maximum value. These results show that the resonance peak moves to shorter wavelengths as the magnitude of the gain is increased. The reader should keep in mind that the values of the absorption efficiencies plotted in Fig. 5(a) may represent either an absorption state, when $Q_{abs} > 0$, or an emission state, when $Q_{abs} < 0$, and that the SR state strictly occurs when the absorption efficiency is negative. The SR state corresponds to the largest value of $|Q_{abs}|$ and occurs at only one wavelength. The change in wavelength is 27.76nm as the gain is varied by one unit. The stair-stepping appearance of Fig. 5(b) is due to the 1nm wavelength simulation resolution; therefore, a change in wavelength is apparent when a shift of more than 1nm occurs. However, the resonance peak corresponds to the lossless SR state at only one particular wavelength, $\lambda = 639nm$, for which the gain reaches, $k = -0.58$, the value needed to excite the SR state in this configuration. The $\{k,\lambda\}$-coordinates of the SR are depicted by the blue crossing lines in Fig 5(b).

#85628 - $15.00 USD Received 23 Jul 2007; revised 21 Aug 2007; accepted 31 Aug 2007; published 17 Sep 2007

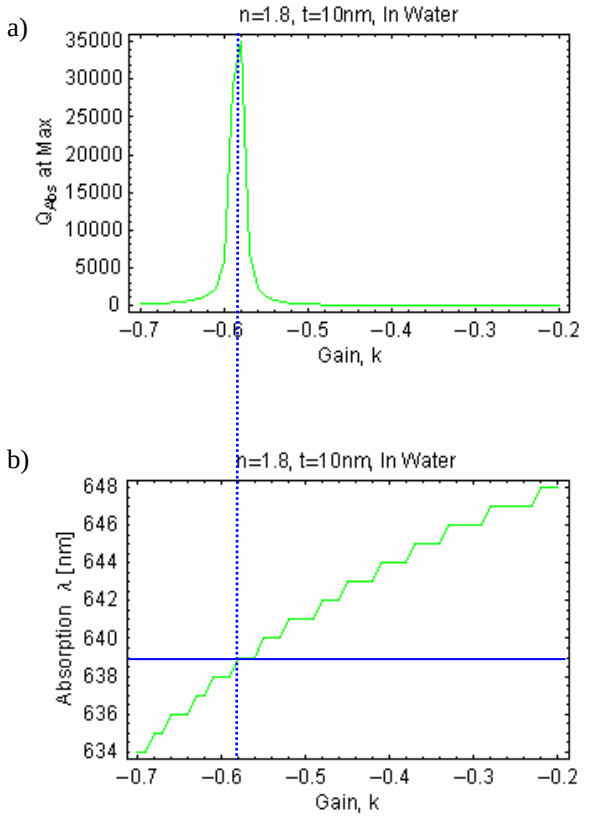

Fig. 5. Determining (a) the gain and (b) wavelength required to excite the super resonant state in the active CNP.

Figure 6 shows the resulting $|Q_{abs}(k,\lambda)|$ spectrum obtained from varying the *index* or the *thickness* of the functional layer of the active CNP when it is immersed in water. The SR peak is identified to show explicitly the trend in the change of gain that is required to excite the SR as the index or thickness is varied. In the first column of subplots the index of the functional layer is varied from n = 1.0 to 2.0; and in the second column the thickness of the functional layer is varied from t = 2.0nm to 10.0nm. As the index or the thickness of the functional layer is varied, the SR state is observed to shift in the amount of gain required to excite it. This property of the SR state is investigated more quantitatively below. Therefore, in a practical application, the amount of pump power required to achieve the appropriate amount of gain in the core of the active CNP that is needed to excite the SR state is a function of the index and the thickness of the functional layer. This indicates that the active CNP may provide a means for sensing nano-scale objects based on a pump power signature. It is possible to envision monitoring the pump power applied to a sample containing functionalized active CNPs while measuring the output power near the SR wavelength. As the pump power is varied, the strength of the output power near the SR wavelength would abruptly increase near the SR state. Any changes in the thickness and or the index of the functional layer, which may result from chemical or nano-scale interactions in the sample that would affect the optical properties or the thickness of the functional layer, could then be remotely detected by monitoring the changes in the pumping power required to excite the SR state.

More quantitatively, the trend in the amount of gain required to excite the SR is explored in detail in Figs. 7-10, where the gain is plotted, respectively, against the thickness and the

#85628 - $15.00 USD Received 23 Jul 2007; revised 21 Aug 2007; accepted 31 Aug 2007; published 17 Sep 2007

index of the functional layer for different background media. These plots show the position of the SR peak in the gain space over the range of values used in the simulations for the index and thickness of the functional layer, keeping the core and the plasmonic layer the same. Results for both the active CNP immersed in air and in water are given. In particular, the gain for the SR as the thickness of the functional layer was varied from 2nm to 10nm in increments of 2nm, for a fixed index $n_3 = 1.7$, is given in Figs. 7 and 8, respectively, when the active CNP is surrounded by air and water. Similarly, the gain for the SR as the index was varied from $n = 1$ to $n = 2$, for a fixed thickness $t = 10nm$, is given in Figs. 9 and 10, respectively, when the active CNP is surrounded by air and water. As before, the peak corresponding to the SR moves to larger gain magnitudes as either the index or the thickness is increased.

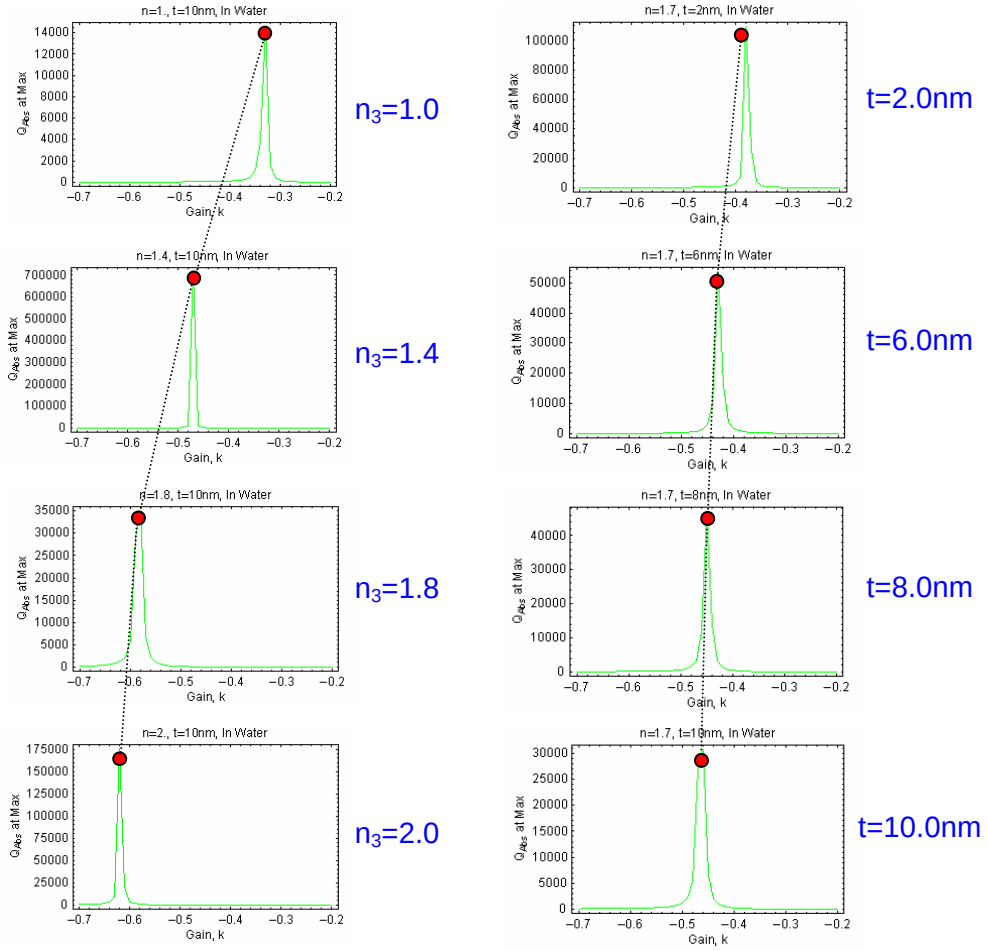

Fig. 6. Trend of gain required to excite the super resonance as the *index* (left column) and *thickness* (right column) of the functional layer is varied.

As the thickness of the functional layer is varied over the range $2nm \le t \le 10nm$, the gain value required to excite the SR state increases in magnitude nearly in a linear fashion. The approximate slopes of this linear relationship are -0.011 for the air environment and -0.0105 for the water environment. Although the slopes are similar between the two cases, the starting gain value in the data set needed to excite the SR state at t = 2nm is greater by -0.21

#85628 - $15.00 USD Received 23 Jul 2007; revised 21 Aug 2007; accepted 31 Aug 2007; published 17 Sep 2007

for the CNP in a water environment as compared to when it is in an air environment. Therefore, the pumping power that would be required to produce the gain needed to excite the SR is larger for an active functionalized CNP in water than one in air.

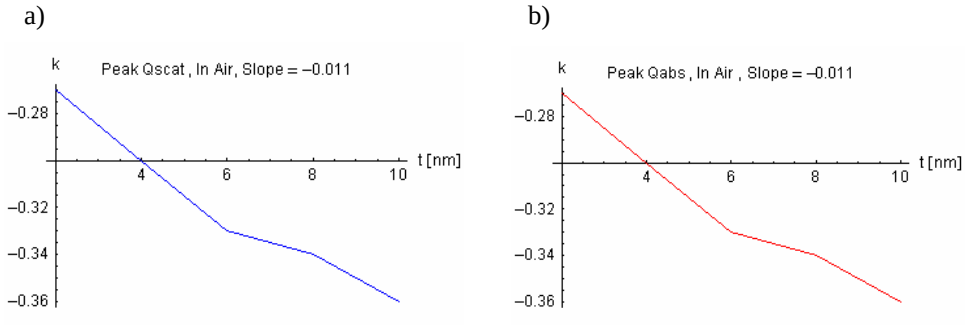

Fig. 7. The gain required to excite the super resonance state for a given functional layer thickness, t, in nanometers and index n=1.7, with the particle in ***air***. The gain and thickness values associated with the super resonance state are given for the peaks of the (a) scattering and (b) absorption efficiencies.

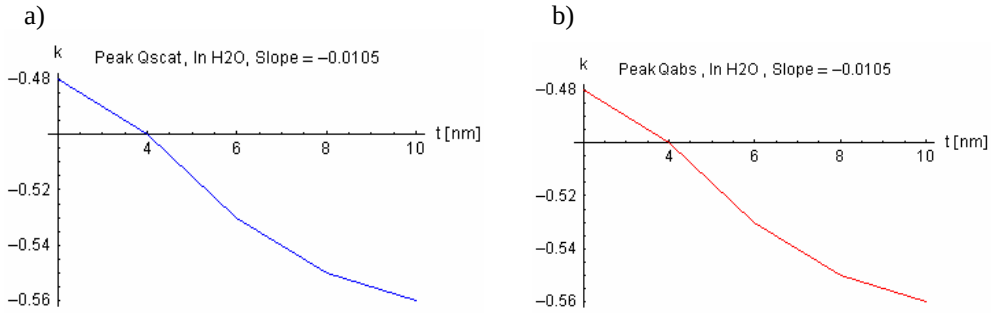

Fig. 8. The gain required to excite the super resonance state for a given functional layer thickness, t, in nanometers and index n=1.7, with the particle in ***water***. The gain and thickness values associated with the super resonance state are given for the peaks of the (a) scattering and (b) absorption efficiencies.

For a finite thickness, $t = 10nm$, functional layer, the gain value required to excite the super resonance state increases in magnitude in a nearly linear fashion as the index of the outer functional layer is varied. These results are shown in Fig. 9 and 10. The approximate slopes of this linear relationship are -0.157 for the air environment and -0.293 for the water environment. This slope behavior is noticeably different from the thickness variation cases. The presence of water surrounding the functionalized CNP changes the slopes by 0.136, which is a significantly larger change then for the case when the thickness of the functional layer was changed. Similarly, the starting gain value at $n = 1$ that is required to excite the SR is larger when the functionalized CNP is in water than in air. The starting value at $n = 1$ when the particle is in an air environment is -0.25 in contrast to -0.33 when it is in a water environment.

#85628 - $15.00 USD Received 23 Jul 2007; revised 21 Aug 2007; accepted 31 Aug 2007; published 17 Sep 2007

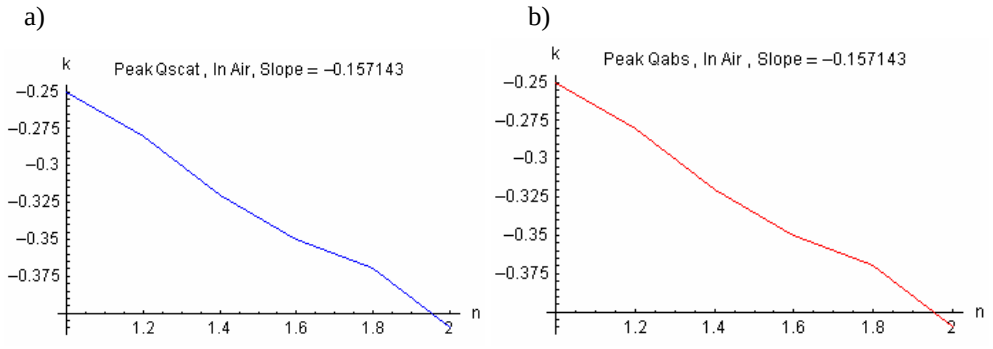

Fig. 9. The gain required to excite the super resonance state for a given functional layer index, n, and thickness, *t=10nm*, with the particle in ***air***. The gain and index values associated with the super resonance state are given for the peaks of the (a) scattering and (b) absorption efficiencies.

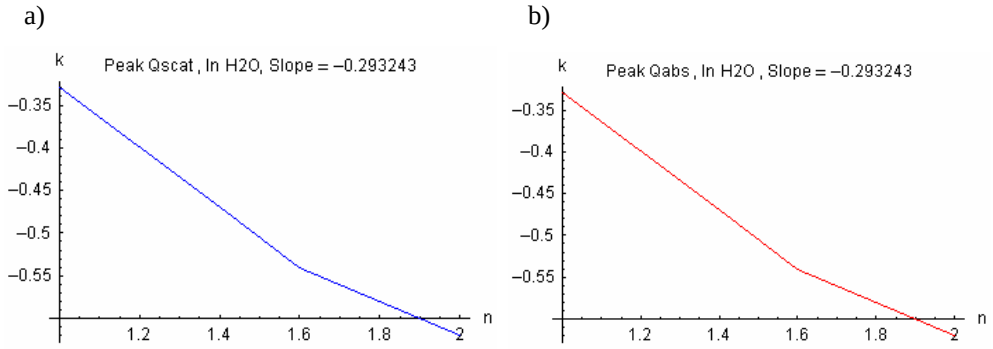

Fig. 10. The gain required to excite the super resonance state for a given functional layer index, n, and thickness, *t=10nm*, with the particle in ***water***. The gain and index values associated with the super resonance state are given for the peaks of the (a) scattering and (b) absorption efficiencies

In addition to sensing nanometer-sized structures, using the active CNP for sensing the global environment may also be desirable. Therefore, the limiting case when the thickness of the functional layer approaches infinity, so that it actually becomes the surrounding medium of the active CNP, was also investigated. In Fig. 11 the gain required to excite the SR state is plotted as a function of the Log (base 10) of the thickness of the functional layer, t, in nanometers with $n_3 = 1.7$, when the background medium was water. Near the point where the thickness increased passed 100nm, there is a departure from the near linear behavior that was observed in Fig. 8 for small thickness layers. As the thickness $t \to \infty$, the gain asymptotically approaches the value $k = -0.81$. This can be attributed to the fact that for small thicknesses the functional layer has a strong affect on the resonance characteristics of the active CNP. However, as the thickness becomes much larger than the CNP, the functional layer appears as the background medium; and, therefore, changes in the thickness of the functional layer have

#85628 - $15.00 USD Received 23 Jul 2007; revised 21 Aug 2007; accepted 31 Aug 2007; published 17 Sep 2007

less and less influence on the resonance characteristics of the CNP. In such a configuration the only influence on the SR state will be due to changes in the surrounding medium index.

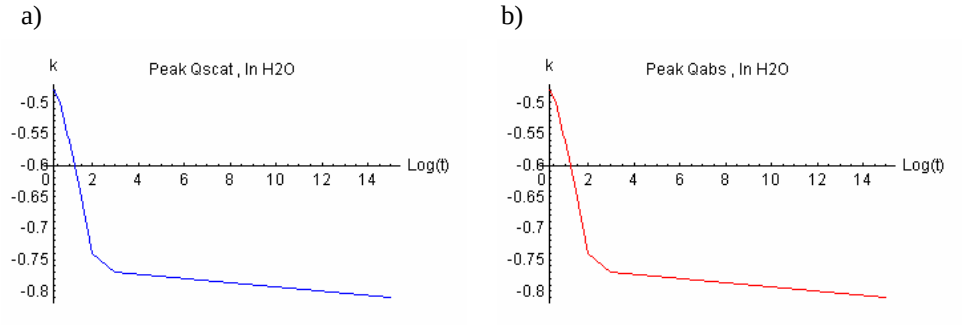

Fig. 11. The gain required to excite the super resonance state for a given functional layer thickness in nanometers, t, and index n=1.7, as $t \to \infty$ with the particle in ***water***. The gain and thickness values associated with the super resonance state are given for the peaks of the (a) scattering and (b) absorption efficiencies.

For the case when the functional layer thickness approaches infinity, the gain required to excite the SR as the index is varied is shown in Fig. 12. In this case the starting gain value at $n = 1$ is -0.25 as was the case for the functionalized particle in air. The final value shown at $n = 2$ is -1.14.

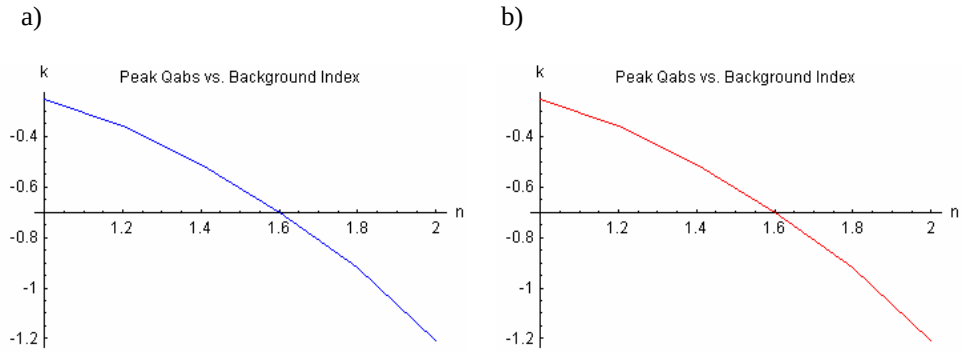

Fig. 12. The gain required to excite the super resonance state for a given functional layer index, n, and infinite thickness with the particle in ***water***. The gain and index values associated with the super resonance state are given for the peaks of the (a) scattering and (b) absorption efficiencies.

Changes in the optical characteristics of the particle as the index or thickness of the functional layer is varied can be investigated by determining the SR resonance wavelength from each of the spectra, $\left|Q_{abs}(k,\lambda)\right|$, as described above and shown in Fig. 6. The resulting values are shown in Figs. 13-16. Figures 13 and 14 and Figs. 15 and 16 show, respectively,

#85628 - $15.00 USD Received 23 Jul 2007; revised 21 Aug 2007; accepted 31 Aug 2007; published 17 Sep 2007

the wavelength variation of the SR as the index and thickness of the functional layer are varied. Figure 13 includes the cases for a functional layer with $t = 10nm$ and for $t = \infty$. In Fig. 13 it is observed that when the surrounding medium is *air*, an index variation in the functional layer with $\Delta n_3 = 1$ increments, shifts the SR wavelength linearly from 502nm to 608nm. Similarly, when the surrounding medium is *water*, the SR wavelength shifts from 528nm to 664nm. Moreover, we note that these two curves are displaced. In particular, for the same functional layer index, the resonance is shifted to longer wavelengths when the active CNP is in water than when it is in air. This is due to the effective wavelength in the surrounding medium being smaller than the free space wavelength by the inverse of the index of the surrounding medium, i.e., because $\lambda_{eff} = \lambda_o / n$. As shown in Fig. 13, when $t = \infty$, the SR wavelength changes linearly but with a larger slope, with the wavelength varying from a value of 502nm to 754nm over the index change, $\Delta n_3 = 1$.

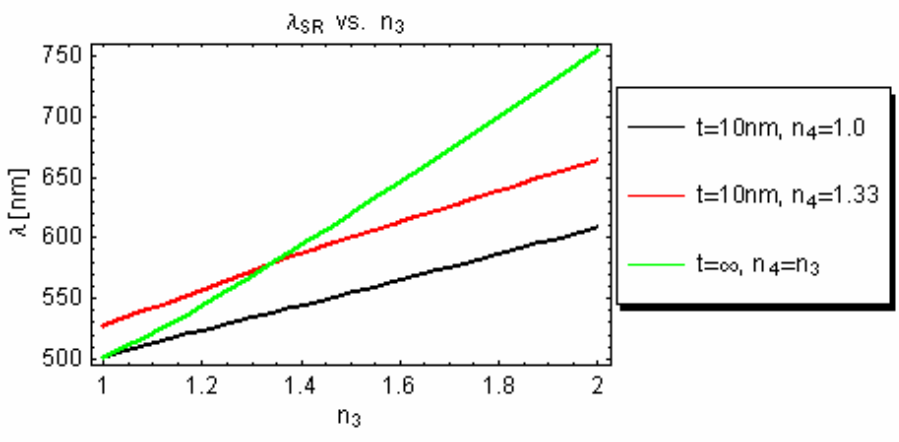

Fig. 13. Super resonance wavelength as the index of the functional layer is varied for thickness values of *t=10nm* for a particle in ***air*** (black) and in ***water*** (red), and for $t \to \infty$ (green).

Figure 14 shows the gain required to excite the SR state for the cases corresponding to the resonance wavelengths given in Fig. 13. It is observed that for a finite thickness of $t = 10nm$, when the index of the functional layer is varied, the SR may occur at the same wavelength for more than one gain value and, thus, for more than one pumping configuration. Therefore, parts of the spectral range covered by $|Q_{abs}(k,\lambda)|$ can be accessed, whether the particle is in air or in water, as the index of the functional layer is varied. For an infinite thickness functional layer, the gain values range from those of the functionalized CNP in air to beyond those of the functionalized CNP in water. Consequently, all wavelengths for the finite thickness cases may be accessed in addition to longer wavelengths not accessible when the functional layer has a finite thickness.

#85628 - $15.00 USD Received 23 Jul 2007; revised 21 Aug 2007; accepted 31 Aug 2007; published 17 Sep 2007

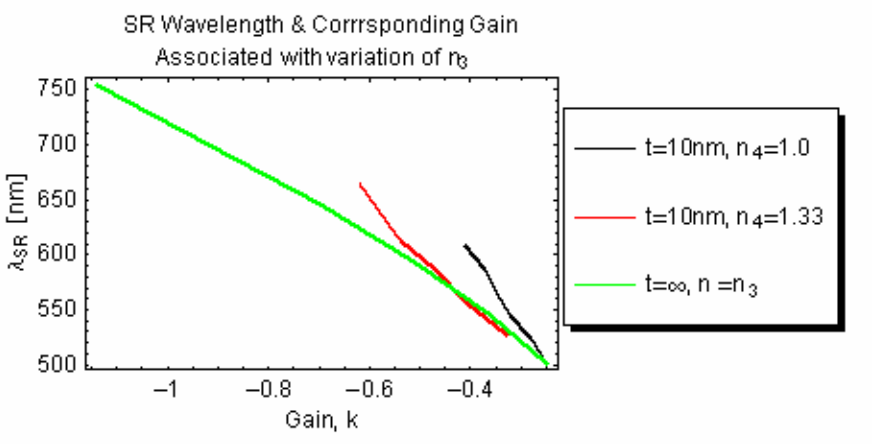

Fig. 14. The gain required to excite the super resonance as the index of the functional layer is varied for thickness values of *t=10nm* for a particle in ***air*** (black) and in ***water*** (red), and for $t \to \infty$ (green).

Upon investigating the spectral dependence of the SR state on the thickness of the functional layer, it is observed in Fig. 15 that when this thickness is varied over a finite amount, the resonance wavelength is tuned to longer wavelengths. In Fig. 15 it is observed that when the surrounding medium is *air*, variations of the thickness of the functional layer from 2nm to 10nm shifts the SR wavelength linearly from 521nm to 576nm; and when the surrounding medium is *water*, they shift the SR wavelength linearly from 528nm to 664nm. Moreover, we note that these two curves are displaced so that for the same functional layer index, the resonance is shifted to longer wavelengths when the particle is in water than when it is in air. As mentioned earlier, this is due to the effective wavelength in the surrounding medium being smaller then the free space wavelength.

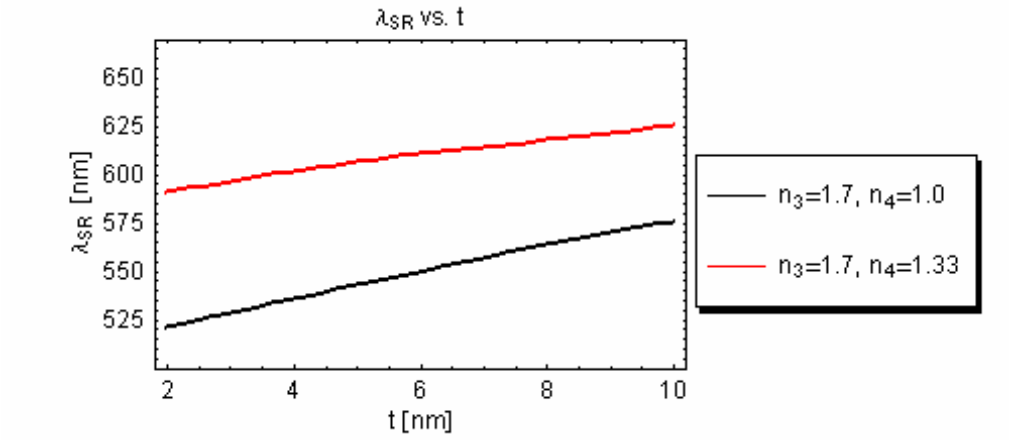

Fig. 15. Super resonance wavelength as the thickness of the functional layer is varied for an index values of $n_3 = 1.7$ for a particle in ***air*** (black) and in ***water*** (red).

Figure 16 shows the gain required to excite the SR state corresponding to the resonance wavelengths given in Fig. 15. It is observed that as the thickness of the functional layer is varied, then up to *t=10nm*, the SR state is separated when the particle is in air or in water so

#85628 - $15.00 USD Received 23 Jul 2007; revised 21 Aug 2007; accepted 31 Aug 2007; published 17 Sep 2007

that the associated wavelengths for the peaks in the spectrum, $|Q_{abs}(k,\lambda)|$, do not over lap and are separated. This behavior is different from that of the index variation shown in Fig. 14, where the SR state may occur at the same wavelength for more than one gain value.

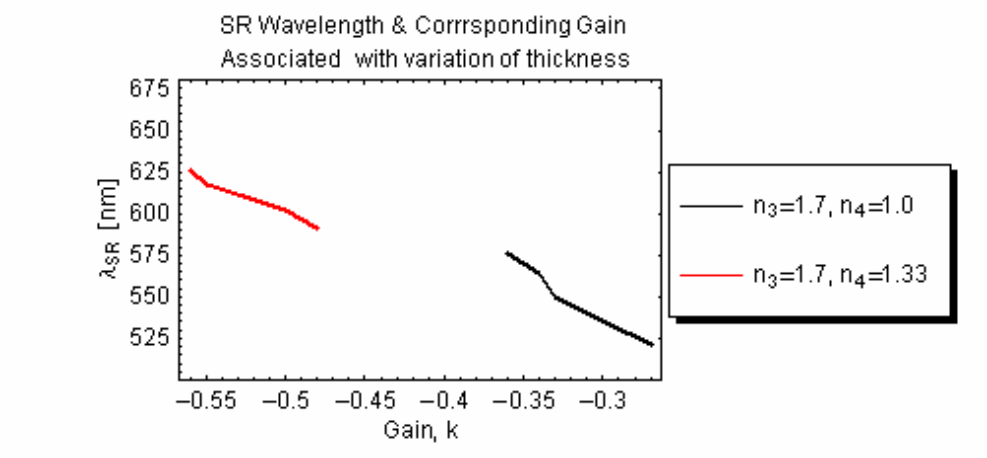

Fig. 16. The gain required to excite the super resonance as the index of the functional layer is varied for an index value of $n_3 = 1.7$ for a particle in ***air*** (black) and in ***water*** (red).

To quantify the performance of the CNP sensor, its *sensitivity* may be calculated for the cases presented above in Figs. 7, 8, 9, 10, 13, and 15. The sensitivity can be defined as the derivative of the measured quantity, i.e., the wavelength or gain *k*, with respect to the quantity of interest, i.e., the refractive index or thickness. The term refractive index unit (RIU) taken to mean one unit of change in the refractive index, and the gain unit (GU) taken to mean one unit of change in the gain, *k*, will be used to specify the sensitivity in the following. From the curves shown in Fig. 13, the sensitivity associated with the SR wavelength dependence on the index n_3 for each curve takes on values of 106.17, 135.22, and 249.24 nm/RIU. These values correspond to the cases when the index of the functional layer is, respectively, 1.0, 1.33, and n_3=n_4. The sensitivity is therefore highest when the CNP is immersed in the medium to be sensed, i.e., when the thickness of the functional layer approaches infinity. From the curves shown in Fig. 15, the sensitivity associated with the thickness of the functional layer in the limit of small layer thickness, i.e., when $t \ll R_3$, takes on values of 6.8 nm/nm and 4.4 nm/nm (although these are *unit-less* quantities, the units are explicitly shown as nm/nm to remind the reader that this is a ratio of wavelength [nm] to thickness [nm]) for the cases of n_3 = 1.0 and n_3 = 1.33, respectively. Therefore, when the wavelength is measured, the sensitivity to thickness changes are two orders of magnitude smaller than when the index of the functional layer are investigated.

If instead the gain is the measured quantity, the sensitivity associated with the gain dependence on the functional layer refractive index and thickness can also be calculated. For the curves in Figs. 7 and 8, which show the gain dependence on the functional layer thickness, the sensitivity is -0.011 GU/nm and -0.0105 GU/nm when the particle is, respectively, in air and water. For the curves in Figs. 9 and 10, which show the gain dependence on the functional layer index, the sensitivity is -0.157 GU/RIU and -0.293 GU/RIU when the particle is in air and water, respectively. Therefore, it *appears* that the sensitivity associated with measuring the SR wavelength is three orders of magnitude larger then its value associated with measuring the gain. However, it must be kept in mind that this

#85628 - $15.00 USD Received 23 Jul 2007; revised 21 Aug 2007; accepted 31 Aug 2007; published 17 Sep 2007

is not a direct comparison. In practice, the gain value would not be measured directly, but rather the pump power required to excite the active core of the CNP sensor into the SR state would be measured. Consequently, the derivative of the gain with respect to pump power must be considered in specifying the gain sensitivity of the CNP sensor. Using the three level rare-earth ion gain model that was developed in [1] for the active core of the CNP, the gain sensitivity in terms of the pump power ratio P (where P is defined as the ratio of the applied pump power to the gain medium threshold pump power), i.e., the sensitivity of the active CNP-based sensor when the pump power is used to interrogate either the index or thickness of the functional layer, may be calculated. The derivative with respect to the gain coefficient when the pump power ratio has the typical value P=10 is $\partial P / \partial k = -146$. Therefore, the gain sensitivity to the thickness of the functional layer at this pump power is $\partial P / \partial t = (\partial P / \partial k)(\partial k / \partial t) \approx 1.66 / nm$ for the CNP immersed in air and 1.53/nm for it immersed in water. The gain sensitivity to the refractive index at this pump power is approximately $\partial P / \partial n = (\partial P / \partial k)(\partial k / \partial n) \approx 22.92 / RIU$ for the CNP immersed in air and 42.78/*RIU* for it immerse in water. Consequently, when the pump power is used for interrogation, the sensitivity to the refractive index of the functional layer is an order of magnitude higher than when the pump power is used to interrogate the thickness of the functional layer. Based on these quantities, the subsequent actual pump power sensitivity will depend on the gain medium pump power, p, not the pump power ratio P. Hence, the pump power sensitivities, defined as $\partial p / \partial n = P_{th}(\partial P / \partial n)$ and as $\partial p / \partial t = P_{th}(\partial P / \partial t)$, will depend on the threshold pump power, P_{th}, of the gain medium used in the core of the active CNP sensor.

Comparing these values to a typical prism or grating coupled SPW sensor near the operating wavelength of 630nm that uses silver for the plasmonic material, and where the index dependence on wavelength is measured, one finds that the sensitivity of the CNP sensor is comparable. When measuring the SR wavelength, the CNP sensor attains sensitivities of at most approximately 249nm/RIU uniformly over operating wavelengths in the range of 500nm to 750nm. In contrast, the prism coupled SPW sensor only does slightly better, attaining sensitivities of approximately 970 nm/RIU [2]. Moreover, the grating coupled SPW sensitivity is even closer to the CNP sensor; it has a sensitivity value of approximately 309nm/RIU [2]. Therefore, there is no drastic loss in sensitivity between the CNP sensor and more traditional SPW-based sensors when the wavelength of the SR state is used in a sensing scheme in order to interrogate the refractive index of a finite or infinite functional layer.

In summary, compared to traditional prism and grating coupled SPW sensors, the active CNP-based sensor has several advantages. It provides a means of realizing a sensor that uses a direct coupling scheme *without* the need for evanescent wave coupling in a nano-meter size. It also allows for highly localized sensing and bio-sensing applications and thus provides a means for *in vivo* sensing. In addition to the wavelength signature, the pump power required to excite the SR state can be used as a signature, thus providing an additional means of interrogating the refractive index or dimensions of the local environment surrounding the CNP. The active CNP-based sensor is capable of sensing with high spatial resolution of index changes within an organism or a biological sample of interest along with high signal strength, both of which lead to a significant increase in the delectability of the characteristics of interest.

5. Analysis of the variations in hemoglobin concentration

Using the model described above and expressed by Eq. (1), the index of the hemoglobin solution can be calculated for different concentrations of hemoglobin (Hb), labeled by C_{Hb}. The dispersive index profile for the Hb solution for different C_{Hb} is shown in Fig. 2. As the C_{Hb} is varied, the index at a particular wavelength is shifted to larger values. Although the dispersion across the wavelength values is non-linear, the index at each wavelength changes

#85628 - $15.00 USD Received 23 Jul 2007; revised 21 Aug 2007; accepted 31 Aug 2007; published 17 Sep 2007

linearly as the C_{Hb} is varied, according to (1). Therefore the changes associated with the SR state are affected linearly by changes in the C_{Hb}.

To better understand the potential of using active CNPs for remote detection of changes in the C_{Hb}, the affects of the C_{Hb} on the wavelength and gain characteristics of the absorption spectrum $|Q_{abs}(k,\lambda)|$ were investigated. For these simulations the optical properties were investigated for an active CNP functionalized by a 10nm thick layer of Hb solution embedded in a water background as well as for an active CNP imbedded in an infinite medium of Hb solution. The influence from changes in the C_{Hb} on the SR wavelength is shown in Fig. 17 for both of these cases. As the C_{Hb} is increased, the resonance wavelength, λ_{SR}, is shifted to larger values in both cases. This behavior is in agreement with the behavior shown in Fig. 13 when the index, n_3, was increased. However for a particular Hb concentration, the SR wavelength is shorter for the case when the finite thickness functionalized layer surrounds the active CNP. Note that there is a one-to-one correspondence between the hemoglobin concentration C_{Hb} and the SR wavelength, λ_{SR}. Exploiting this one-to-one relationship could provide a means for determining the C_{Hb} remotely, i.e., by merely measuring the narrow emission of a sample that contains functionalized active CNPs or has been imbedded with active CNPs.

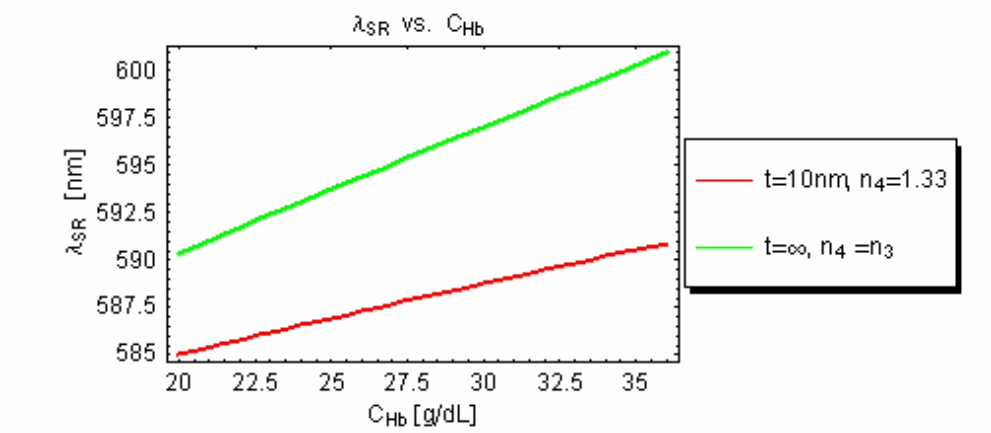

Fig. 17. Super resonance wavelength as the concentration of hemoglobin, C_{Hb}, of the functional layer is varied for thickness values of *t=10nm* for a particle in ***water*** (red), and for $t \to \infty$ (green).

The effects on the gain required to excite the SR were also investigated as the C_{Hb} was varied. These results are shown in Fig. 18. As the C_{Hb} is increased, the amount of gain required to excite the SR increases. This behavior is due to the dependence of the SR wavelength λ_{SR} and gain k on the index, n_3, as was demonstrated above and shown in Figs. 13 and 14. As mentioned before, the linear dependence of the index of the hemoglobin solution on the C_{Hb} is responsible for the linear characteristics associated with the SR excitation gain and wavelength variations.

#85628 - $15.00 USD Received 23 Jul 2007; revised 21 Aug 2007; accepted 31 Aug 2007; published 17 Sep 2007

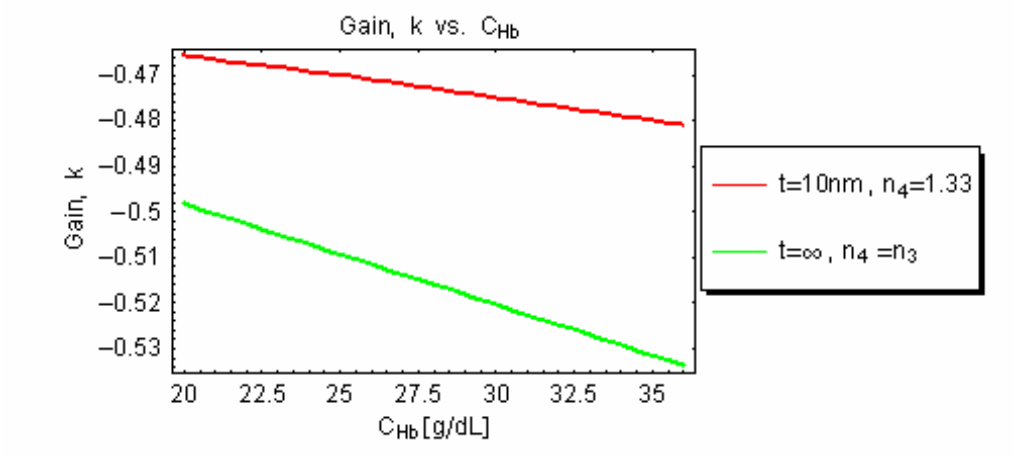

Fig. 18. The gain required to excite the super resonance as the concentration of hemoglobin, C_{Hb} , of the functional layer is varied for thickness values of *t=10nm* for a particle in ***water*** (red), and for $t \to \infty$ (green).

As was shown for the relationship between the λ_{SR} and C_{Hb}, there also exists a one-to-one relationship between the gain *k* needed to excite the SR and the hemoglobin concentration C_{Hb}. This behavior is also illustrated in Fig. 18 where the magnitude of gain required for the case with *t=10nm* is less than for the case when $t \to \infty$. It indicates that in addition to using the emission wavelength of the SR state, the pumping power required to achieve the gain needed to excite the SR may also be exploited to remotely detect the concentration of hemoglobin in the outer layer of the functionalized active CNP particle. Therefore, the measurement of the excitation wavelength and/or of the pump power required to excite the SR provides a direct way to determine the hemoglobin concentration C_{Hb} remotely.

6. Conclusions

In this paper we investigated the use of active CNPs for nano-sensing applications. We presented simulation results of the optical properties of an active CNP with a 24nm radius active silica core and 6nm thick silver shell that has been functionalized by an additional spherical outer layer of varying thickness and refractive index. Simulation results showing the effects of the functionalized layer thickness and index on the super-resonant (SR) state of the active CNP are presented. It was shown that the wavelength and amount of optical gain required to excite the SR state provides *both* a spectral and a power signature which may be used to identify the dimensions and optical properties of the functionalized layer. The performance of the CNP sensor was compared to more traditional large planar prism and grating plasmonic sensors based on surface plasmon waves; it was shown that the active CNP-based sensor provides approximately the same level of sensitivity when the wavelength is used for interrogation. It was all so shown that the signature associated with varying the pump power required to excite the gain medium to achieve the SR state in the CNP sensor provides an additional means for interrogation with modest sensitivity. Thus, given its localized nature and its direct excitation mechanism, the active CNP-based sensor has some advantages over more traditional SWP-based sensor systems. Finally these results were applied to the case of a functionalized layer containing a solution of human hemoglobin. It is shown that by determining the wavelength and gain required to excite the super resonance state of the CNP in the presence of the hemoglobin solution, the concentration of hemoglobin may be determined.

#85628 - $15.00 USD Received 23 Jul 2007; revised 21 Aug 2007; accepted 31 Aug 2007; published 17 Sep 2007

Acknowledgments

This work was supported in part by DARPA Contract number HR0011-05-C-0068.

#85628 - $15.00 USD Received 23 Jul 2007; revised 21 Aug 2007; accepted 31 Aug 2007; published 17 Sep 2007